Carbohydrate Polymers 148 (2016) 300–308

Contents lists available at ScienceDirect

Carbohydrate Polymers

journal homepage: www.elsevier.com/locate/carbpol

Synthesis of polyvinyl alcohol/cellulose nanofibril hybrid aerogel microspheres and their use as oil/solvent superabsorbents

Tianliang Zhai[a,b], Qifeng Zheng[c,d], Zhiyong Cai[e], Hesheng Xia[a,*], Shaoqin Gong[b,c,d,**]

[a] State Key Laboratory of Polymer Materials Engineering, Polymer Research Institute, Sichuan University, Chengdu 610065, China
[b] Department of Biomedical Engineering, University of Wisconsin, Madison, WI 53715, United States
[c] Department of Material Science and Engineering, University of Wisconsin, Madison, WI 53715, United States
[d] Wisconsin Institute for Discovery, University of Wisconsin, Madison, WI 53715, United States
[e] Forest Product Laboratory, USDA, Madison, WI 53726, United States

ARTICLE INFO

Article history:
Received 3 January 2016
Received in revised form 28 March 2016
Accepted 14 April 2016
Available online 19 April 2016

Keywords:
Aerogel microspheres
Cellulose nanofibrils (CNFs)
Emulsification process
Freeze-drying
Superabsorption

ABSTRACT

Superhydrophobic and crosslinked poly(vinyl alcohol) (PVA)/cellulose nanofibril (CNF) aerogel microspheres were prepared via a combination of the water-in-oil (W/O) emulsification process with the freeze-drying process, followed by thermal chemical vapor deposition of methyltrichlorosilane. The oil phase and the cooling agent were judiciously selected to ensure that the frozen ice microspheres can be easily separated from the emulsion system. The silanized microspheres were highly porous with a bulk density ranging from 4.66 to 16.54 mg/cm^3. The effects of the solution pH, stirring rate, and emulsifier concentration on the morphology and microstructure of the aerogel microspheres were studied. The highly porous structure of the ultralight aerogel microspheres demonstrated an ultrahigh crude oil absorption capacity (up to 116 times its own weight). This study provides a novel approach for the large-scale preparation of polymeric aerogel microspheres with well-controlled particle sizes that can be used for various applications including oil and chemical spill/leak clean-up.

1. Introduction

Aerogels, a family of highly porous solid materials, possess a number of unique characteristics including ultralow density, high specific surface area, and high porosity, as well as excellent thermal, acoustic, and dielectric properties (Husing & Schubert, 1998; Kistler, 1931; Wu, Xu et al., 2012). Therefore, aerogels can be potentially used for various applications including absorbents (Bi et al., 2012; Zheng, Cai, & Gong, 2014), supercapacitors (Bi et al., 2012; Zheng, Cai, Ma, & Gong, 2015), energy storage (Su et al., 2013), gas sensors (Yavari, Chen, Thomas, Ren, Cheng, & Koratkar, 2011), and catalysis supports (Wu, Yang et al., 2012). However, research on aerogels, particularly polymer-based aerogels, over the past few decades has been mainly focused on monolithic aerogels (Aegerter, Leventis, & Koebel, 2011; Antonietti, Fechler, & Fellinger, 2014). Reports on polymer-based microspherical aerogels are rare (Alnaief, Alzaitoun, Garcia-Gonzalez, & Smirnova, 2011; Cai et al., 2014; Garcia-Gonzalez & Smirnova, 2013).

Microspherical aerogels offer additional desirable features over their bulky counterparts, such as controllable particle sizes and tailorable pore structures, as well as alterable physical and chemical properties. Therefore, microspherical aerogels, mostly non-polymer based, have been explored for many applications including as cell culture templates (Cai et al., 2014), superabsorbents (Yun, Luo, & Gao, 2014), drug delivery templates (Vazhayal, Talasila, Azeez, & Solaiappan, 2014), supercapacitors (Liu, Zhang, Fu, Dresselhaus, & Dresselhaus, 2006), etc. Due to the unique structure of aerogels, it is impossible to obtain spherical microparticles from monolithic aerogels via crushing or milling (Cai et al., 2014). Microspherical aerogels are typically derived from the production of polymeric microspheres followed by appropriate drying processes. The microsphere formation step determines the shape and size of the resulting microspheres, while the subsequent drying step controls the porous structure. Supercritical drying (El Kadib & Bousmina, 2012) and freeze-drying(Chen, Yu, Li, Liu, & Li, 2011) are the two most commonly used drying methods in the production of polymer-based aerogels.

Generally, aerogels prepared using the supercritical drying process possess a very high specific surface area and small pore sizes.

* Corresponding author.
** Corresponding author at: Department of Biomedical Engineering, University of Wisconsin, Madison, WI 53715, United States.
E-mail addresses: xiahs@scu.edu.cn (H. Xia), sgong@engr.wisc.edu (S. Gong).

http://dx.doi.org/10.1016/j.carbpol.2016.04.065
0144-8617/

Alnaief et al. (2011) prepared an alginate microspherical aerogel using the sol-gel process combined with the emulsion method followed by supercritical drying. The Burnauer–Emmett–Teller (BET) surface areas of these alginate aerogel microspheres were in the range of 318–680 m^2/g. However, the supercritical drying process is time-consuming and expensive (Hong, Yoon, & Hwang, 2012). In contrast, the freeze-drying process is safe, less expensive, and efficient. Cai et al. (2014) recently employed a spray-freeze-drying method to prepare ultralight cellulose nanofibril (CNF) aerogel microspheres for cell culture applications. This method does not involve any potentially toxic solvents to produce microspherical aerogels; however, there was only limited control over the particle size and distribution of the resulting aerogel microspheres.

The emulsification process, which is frequently used to prepare polymeric microspheres, can enable large-scale production of microspheres with controllable particle sizes and distributions (Okubo, Katayama, & Yamamoto, 1991; Okubo, Shiozaki, Tsujihiro, & Tsukuda, 1991). Therefore, the combination of the emulsification process with the freeze-drying process can potentially offer an efficient fabrication process to produce customizable microspherical aerogels. However, to date, we have not found any relevant report utilizing such a process to produce polymeric aerogel microspheres. The rarity of such work may be attributed to the fact that the emulsification process typically requires the use of organic solvents; while the freeze-drying process is a very efficient and safe way to remove water, it is often less efficient and more hazardous to remove organic solvents.

Here we present a new fabrication method combining the water-in-oil (W/O) emulsion process with the freeze-drying technique to prepare poly(vinyl alcohol) (PVA)/cellulose nanofibril (CNF) aerogel microspheres. CNFs are derived from cellulose, the most abundant renewable natural polymer, and are biodegradable and biocompatible (Klemm, Heublein, Fink, & Bohn, 2005). Moreover, CNFs all exhibit outstanding mechanical properties (Klemm et al., 2011; Moon, Martini, Nairn, Simonsen, & Youngblood, 2011). To address the aforementioned challenges related to removing organic solvents via freeze-drying, we judiciously chose to use toluene with a freezing point of −95 °C as the oil phase during the emulsion process and a dry ice/acetone solution with a freezing point of −78 °C as the cooling agent during the initial freezing process conducted before the freeze-drying process to ensure that the aqueous phase can be completely frozen while the oil phase still remains in a liquid state. Subsequently, the resulting suspension of the frozen water droplets, containing both PVA and CNFs, in the oil phase (i.e., toluene) can be conveniently filtered to remove the oil phase before the freeze-drying process, thereby eliminating the need to remove the organic solvent during the freeze-drying process. Water pollution from oil and chemical spills/leaks arising from accidents or disasters is catastrophic for aquatic ecosystems (Adebajo, Frost, Kloprogge, Carmody, & Kokot, 2003).There is a growing demand for innovative absorptive materials with high absorption capacities and efficiencies. In the present work, the hydrophobic PVA/CNF aerogel microspheres were obtained by silane treatment. The PVA/CNF aerogel microspheres demonstrated superior oil absorption capacities and were capable of removing floating oil.

2. Experimental

2.1. Materials

Bleached eucalyptus Kraft pulp purchased from Fibria Celulose was used as the raw material for preparing the CNFs. Polyvinyl alcohol (PVA, M_w: 89,000–98,000 g/mol, >99% hydrolyzed), methyltrichlorosilane (99 wt%), Span-80, and 2,2,6,6,-tetramethyl-1-piperidinyloxy (TEMPO, 98 wt%) were all obtained from Sigma–Aldrich. 1,2,3,4,-butanetetracarboxylic acid (BTCA) (purity >98%) was acquired from Acros Organics, USA. Sodium hypophosphite monohydrate ($NaPH_2O_2{\cdot}H_2O$) was purchased from Alfa Aesar, USA. Sodium bromide, sodium chlorite, sodium hypochlorite solution, hydrochloric acid, and other chemicals were of laboratory grade (Fisher Scientific, USA) and used without further purification.

2.2. Preparation of CNFs

The TEMPO-oxidized CNFs used in this work were produced according to the procedures reported by Isogai's group (Saito, Hirota, Tamura, Fukuzumi, & Isogai, 2009). Fully bleached eucalyptus fibers were oxidized with sodium hypochlorite using 2,2,6,6,-tetramethyl-1-piperidinyloxy (TEMPO) as a catalyst at a temperature of 60 °C for 48 h. The resulting fibers were then thoroughly washed and refined in a disk refiner with a gap of approximately 200 μm. The coarse fibers were separated by centrifuging at 12000 G, and the fine CNF dispersion was then concentrated to 0.74 wt% using ultrafiltration. The nanofiber suspension was then refined by passing through an M-110EH-30 microfluidizer (Microfluidics, Newton, MA) once with 200- and 87-μm chambers in series. The resulting CNF suspension was stored at 4 °C without any treatment before future utilization.

2.3. Preparation of BTCA/$NaPH_2O_2$ solution

BTCA (100 mg) and $NaPH_2O_2{\cdot}H_2O$ (50 mg) were dissolved in water and diluted with water to 100 mL in a 100 mL volumetric flask.

2.4. Preparation of PVA/CNF aqueous solution

The PVA solution (8 mL, 0.1 g/mL), CNF suspension (108 g, 0.74 wt%), BTCA/$NaPH_2O_2$ solution (8 mL), and DI water (124 mL) were mixed in a 500 mL three-necked flask under moderate mechanical stirring for 1 h. The weight ratio between the PVA and CNF was fixed at 1:1. Dilute sulfuric acid (pH = 1) or sodium bicarbonate solution (pH = 13) were then added into the flask in order to adjust the pH of the solution to the desired value (4.0, 4.6, and 4.9). After degassing, the PVA/CNF aqueous solution was sealed in a conical flask for future use.

2.5. Preparation of crosslinked PVA/CNF microspherical aerogels

Toluene (450 mL) and Span 80 (0.5, 1.0, 1.5, or 2.0% of the aqueous phase) were mixed to serve as the oil phase. Under a desired stirring speed (500, 750, or 1000 rpm), PVA/CNF aqueous solution (50 mL) was added dropwise into the oil phase at a volume ratio of 1:9 (aqueous solution to oil) to produce the water-in-oil (W/O) emulsion. The resulting emulsion was continuously stirred for 1 h and subsequently cooled in a dry ice/acetone solution (−78 °C) bath for 20 min. During this initial freezing process prior to the freeze-drying process, the aqueous droplets containing PVA and CNFs were completely frozen and formed ice microspheres; however, the oil phase, namely, toluene with a freezing point of −95 °C, remained as a liquid at this temperature. Thereafter, the ice microspheres were separated from the oil phase by simple filtration and were then washed by hexanes (−40 °C). The washed ice microspheres were freeze-dried immediately in a lyophilizer at a condenser temperature of −87 °C under vacuum (0.0014 mbar) for three days to produce uncrosslinked aerogel microspheres. Finally, the aerogel microspheres were crosslinked after they were heated at 140 °C for 5 min to allow completion of the crosslinking reaction. The syn-

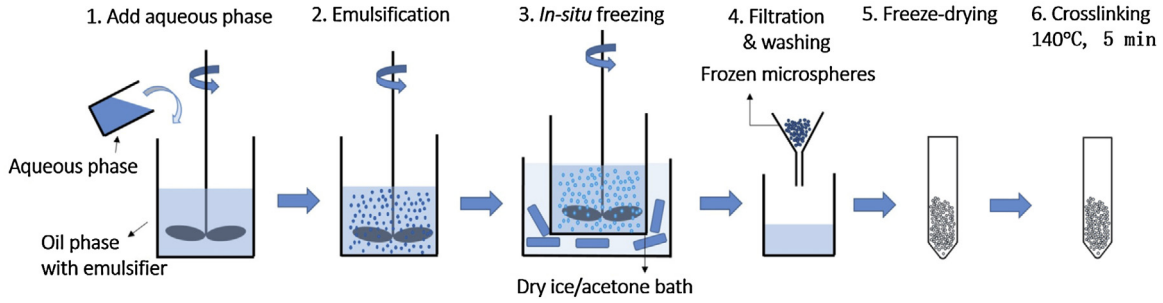

Fig. 1. Schematic description of the synthesis route of the PVA/CNF aerogel microspheres via the emulsification process combined with freeze-drying.

thesis route of the PVA/CNF aerogel microspheres is schematically shown in Fig. 1.

2.6. Preparation of hydrophobic PVA/CNF microspherical aerogels

A thermal chemical vapor deposition (CVD) method was used for the surface modification of the PVA/CNF aerogel microspheres (Zheng et al., 2014). Methyltrichlorosilane (1 mL) stored in a glass vial and PVA/CNF aerogel microspheres (~200 mg) stored in a 50 mL centrifuge tube were placed in a vacuum desiccator. The desiccator was then vacuumed to 80 kPa below atmospheric pressure and heated inside of a 50 °C oven for 48 h. After the silanization reaction was complete, nitrogen gas was flushed into the desiccator to remove any excess unreacted silane and by-products.

2.7. Characterization

For each type of characterization described below, unless otherwise stated, at least three specimens were measured for each data point and the average results were reported. The bulk densities of the aerogel microspheres were calculated by measuring the mass and volume of the aerogel microspheres. The morphology and microstructure of the aerogel microspheres were investigated using a scanning electron microscope (SEM, LEO GEMINI 1530). The microspherical aerogels were blown out of the container and fell onto the carbon tape separately. The surface of the microspherical aerogels was then treated by gold sputtering. The Brunauer–Emmett–Teller (BET) specific surface area was determined by N_2 physisorption using a Gemini VII analyzer (Micromeritics Instruments, USA). The FTIR spectra were obtained on a Tensor 27 spectrometer (Bruker Daltonics Inc., USA) with 4 cm^{-1} resolution at room temperature. Thermal stability measurements were carried out using a thermogravimetric analyzer (TGA, Q50 TA Instruments, USA) from 30 to 800 °C at a 10 °C min^{-1} heating rate under N_2 protection. The samples were pretreated at 100 °C for 1 h to remove moisture before the TGA tests.

The density of the solid materials (ρ_s) was calculated based on the solid density of each component and their weight ratios according to Equation (1):

$$\rho_s = \frac{1}{\left(W_{silane}/\rho_{silane}\right) + \left(W_{CNF}/\rho_{CNF}\right) + \left(W_{PVA}/\rho_{PVA}\right)} \quad (1)$$

where W is the weight percentage of the different components, and ρ_{CNF}, ρ_{PVA}, and ρ_{silane} are the solid densities of CNF, PVA, and silane, respectively. The densities of the CNF, PVA, and silane used for this study were 1460, 1269, and 1273 kg m^{-3}, respectively, according to the manufacturer's data sheet.

The porosity (P) of aerogel microspheres was calculated according to Eq. (2):

$$P(\%) = \left(1 - \rho/\rho_s\right) \times 100\% \quad (2)$$

where ρ is the density of the aerogel, and ρ_s is the density of the solid material.

2.8. Oil/solvent absorption capacity measurements

To measure the oil/solvent absorption capacities of the aerogel microspheres, the silane-coated microspheres (~10 mg) were put into a small glass vial of which the weight was measured and recorded before use. The oil/solvent was added dropwise into the vial containing microspheres using a dropper. The absorption process was very fast. A new drop of oil/solvent was added once the previous drop was completely absorbed. The addition of oil/solvent droplets were stopped once the maximum absorption capacity was reached. The maximum absorption capacity was reached when a tiny oil/solvent liquid flow appeared after the glass vial was turned upside-down. The absorption capacity (Q) was calculated from the mass gain using Eq. (3),

$$Q(\%) = \frac{(W - W_0)}{W_0} \times 100 \quad (3)$$

where W and W_0 are the weights of the aerogel microspheres before and after absorption, respectively. For each test, 5 parallel samples were used and the average value of absorption capacity with standard deviation were reported.

3. Results and discussion

3.1. Formation of PVA/CNF aerogel microspheres

Emulsification is a well-known process that can allow for the large-scale production of microspheres. Meanwhile, freeze-drying is a safe, less expensive, and efficient drying technique that can be used to form aerogels. The combination of these two techniques is a promising method for producing highly porous aerogel microspheres. Fig. 1 shows the schematic fabrication process for the PVA/CNF aerogel microspheres combining the emulsification and freeze-drying techniques. In order to develop a "green" and simple process, several strategies were employed. First, by judiciously selecting the oil phase (organic solvent) and the cooling agent for the emulsion solution (Step 3 in Fig. 1) with different freezing points, the oil phase required for the emulsification process can be conveniently removed from the resulting emulsion solution via filtration after the initial freezing process prior to freeze-drying, thereby avoiding the need to remove any organic solvent by freeze-drying. In this study, toluene with a freezing point of −95 °C and dry ice/acetone solution with a freezing point of −78 °C were chosen as the oil phase and cooling agent used to freeze the emulsion solution prior to freeze-drying, respectively. Due to the freezing point difference between the oil phase and the aqueous phase, frozen ice microspheres containing PVA and CNFs can be readily formed during the freezing process prior to the freeze-drying pro-

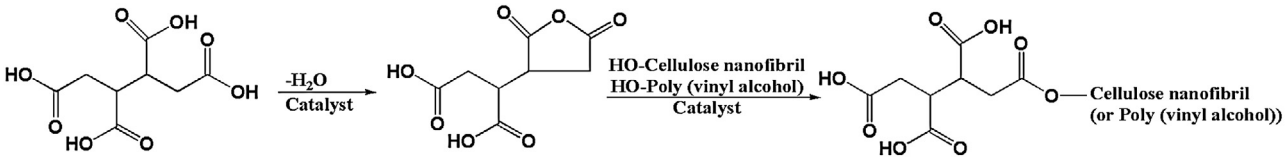

Fig. 2. Esterification of the hydroxyl groups present on PVA molecules and CNFs with BTCA.

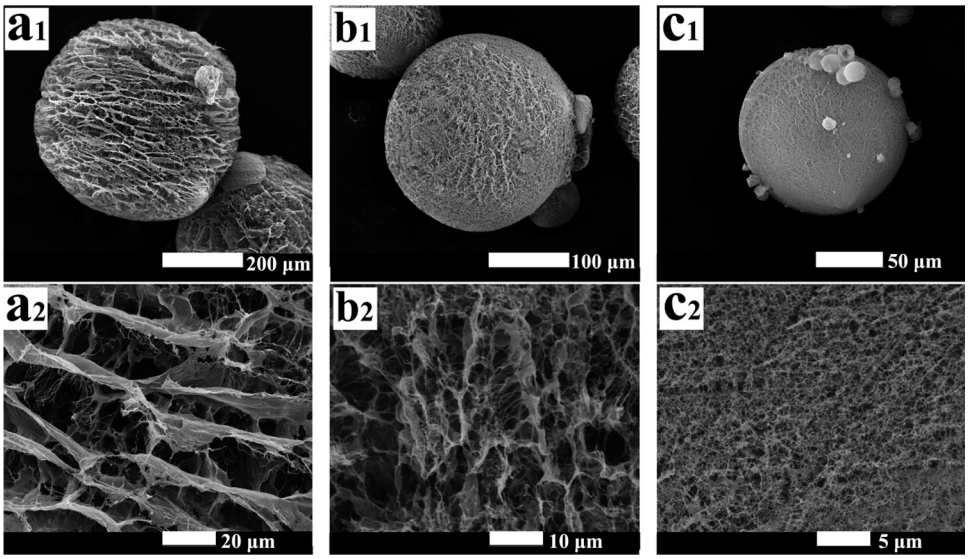

Fig. 3. Typical SEM images of the PVA/CNF aerogel microspheres prepared using different stirring rates: (a_1) and (a_2) 500 rpm, (b_1) and (b_2) 750 rpm, and (c_1) and (c_2) 1000 rpm. The scale bars for (a1), (b1), (c1), (a2), (b2), and (c2) were 200, 100, 50, 20, 10, and 5 μm, respectively.

cess, while keeping the oil phase (toluene) in its liquid form. As such, the oil phase and the frozen ice microspheres can be easily separated via filtration (Step 4 in Fig. 1). Secondly, crosslinking the aerogel microspheres can enhance their mechanical properties and improve their stability in various liquid media. In this study, instead of using a crosslinking agent such as glutaraldehyde that reacts in an aqueous solution and may also require a relatively long reaction time, we chose to use the crosslinking agent BTCA, which can react in a solid state instead of a solution thereby simplifying the process. BTCA is a well-known nontoxic, formaldehyde-free, polyfunctional crosslinking agent for fluff pulp crosslinking (Feczko, Kokol, & Voncina, 2010; Lund & Brelid, 2013). It has four carboxylic acid groups that can form ester bonds with the abundant hydroxyl groups present on PVA and CNFs. Esterification can be achieved by heat treatment and generally salts of weak acids are used as catalysts for acceleration of the reaction (Cay & Miraftab, 2013). The reaction of BTCA with hydroxyl groups is usually described as proceeding via a cyclic anhydride intermediate as shown in Fig. 2 (Harifi & Montazer, 2012). Therefore, by using BTCA as the crosslinking agent, the crosslinking reaction condition of the aerogel microspheres can be rather simple. Namely, the freeze-dried aerogel microspheres were crosslinked after being heated at 140 °C for 5 min.

The morphology and size distribution of the aerogel microspheres produced by the combined emulsification and freeze-drying processes can be influenced by many factors, such as the water-to-oil ratio, stirring rate, type of surfactant, and viscosity, etc. (Alnaief et al., 2011). In this work, the effects of three processing parameters on the morphology and size distribution of the aerogel microspheres were investigated including the pH value of the PVA/CNF solution, emulsifier concentration, and stirring rate.

3.2. Effect of the pH value of the PVA/CNF solution on the morphology of the aerogel microspheres

To prepare the aerogel microspheres with various particle sizes and a well-defined spherical shape, the experimental parameters, such as pH value of the PVA/CNF solution, emulsifier concentration and stirring rate were optimized successively. The CNFs prepared by the TEMPO-oxidation method were dispersed in an alkaline aqueous suspension because deprotonated carboxylate groups present on the TEMPO-oxidized CNFs can improve the water suspension stability of the CNFs in an alkaline environment (Saito, Kimura, Nishiyama, & Isogai, 2007). However, when the sodium carboxylate groups present on the TEMPO-oxidized CNFs are converted to free carboxyl groups by ion-exchange in an acid environment, much stronger hydrogen bonding between the CNF and PVA molecules can be formed which can help to enhance the stability of the water droplets (i.e., the liquid microspheres) containing the PVA and CNFs during the emulsification process. To study the effects of the pH value of the PVA/CNF solution on the morphology of the resulting aerogel microspheres, three different pH values, namely, 4.0, 4.6, and 4.9, were investigated. The pH of the PVA/CNF solution was 4.6 because the crosslinker (i.e., BTCA) was acidic and was mixed into the PVA/CNF solution before the emulsification process. The other two pH values, namely, 4.0 and 4.9, were obtained by adding a dilute base or acid, respectively. The surfactant content was fixed at 1.0% and the stirring rate used for this study was 1000 rpm. Fig. S1 shows the SEM images of the aerogel microspheres prepared from the PVA/CNF solution with different pH values. The variation of the pH value did not show an obviously influence on the particle size of the microspheres. But it is clear shown that the aerogel microspheres prepared from

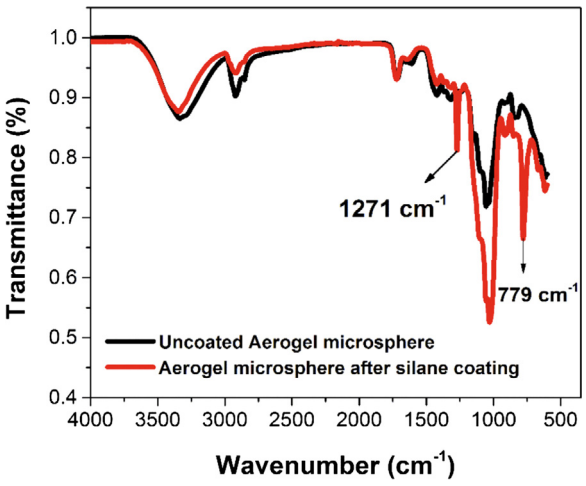

Fig. 4. FTIR spectra of the PVA/CNF aerogel microspheres with and without silane coating.

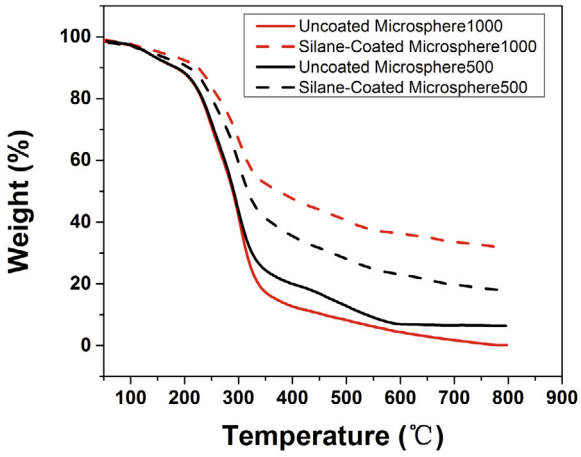

Fig. 5. TGA curves of the PVA/CNF aerogel microspheres with and without silane coating.

the PVA/CNF solution with a lower pH value (pH 4.0) had a more spherical shape (Fig. S1(c_1) and (c_2)) in comparison with the microspheres made from PVA/CNF solutions with higher pH values, (e.g., Fig. S1(a_1) and (a_2) for pH 4.9 and Fig. S1(b_1) and (b_2) for pH 4.6). This phenomenon indicated that stronger hydrogen bonds formed in an acidic condition could dramatically improve the stability of the liquid microspheres under vigorous stirring. However, with a decreasing pH value, the viscosity of the PVA/CNF solution significantly increased, which led to degassing difficulties during the preparation of the PVA/CNF solution. Therefore, the pH of the PVA/CNF solution was optimized to 4.0 for all other studies.

3.3. Effect of the emulsifier concentration

Span-80 was used as the emulsifier/surfactant during the emulsification process to prevent coalescence of the droplets. Four different emulsifier concentrations were investigated in this study, namely, 0.5%, 1.0%, 1.5%, and 2.0%. The concentration of the emulsifier was the weight percentage of the emulsifier relative to the weight of the aqueous phase (i.e., the PVA/CNF solution). The pH value of the PVA/CNF solution was fixed at 4.0 as discussed earlier. The stirring rate was set at 1000 rpm. As shown in Fig. S2, spherical aerogel microspheres could not be obtained when the emulsifier concentration was below 1.0%. Table S1 provides the average particle sizes of the aerogel microspheres prepared using different emulsifier concentrations. The average particle size of the aerogel microspheres decreased from 54 to 31 μm when the emulsifier concentration increased from 1.0% to 2.0%. This can be attributed to the fact that higher concentrations of emulsifier can minimize the interfacial surface tension between the aqueous phase and the oil phase. Despite the fact that the variation of particle size can be achieved by varying the emulsifier concentration, the particle size difference was relatively small. Moreover, high emulsifier concentrations could lead to the emulsifier removing difficulties. To remove the emulsifier from the frozen microspheres, the microspheres were washed by abundant hexanes (−40 °C) multiple times before freeze-drying. Because the emulsifier (Span-80) was soluble in hexane at −40 °C, thus, most of it was washed away. However, at a higher emulsifier concentration, it may be possible that a small fraction of the emulsifier still stuck on the microspheres' surface because a longer dissolving time was needed. This would lead to a residue emulsifier problem. As shown in Fig. S2(b) and (c), the aerogel microspheres formed with an emulsifier concentration of 1.0% and 1.5% could be individually separated by blowing (see the SEM Experiment section). However, the microspheres formed with 2.0% emulsifier tended to form aggregates (Fig. S2(d)). To minimize the chance of a residue emulsifier problem, the emulsifier concentration was set to 1.0% for the rest of the studies.

3.4. Effect of the stirring rate

As shown in Fig. S3, the size of the aerogel microspheres decreased dramatically when the stirring rate increased from 500 to 1000 rpm, indicating that the stirring rate had a significant influence on the morphology of the microspheres. The values of the particle sizes and several other properties are listed in Table 1. The numbers appearing in the sample names represent the corresponding stirring rate. For example, Microsphere500 refers to the microspheres prepared under 500 rpm. The particle size decreased from 499 to 53 μm as the stirring rate increased from 500 to 1000 rpm. A higher stirring rate leads to a higher energy input to the emulsion system, which helps to generate a larger interfacial surface area, and hence, smaller droplets (Alnaief et al., 2011). However, when the stirring rate increased to 1500 rpm, no microspheres with a desirable spherical shape were obtained. This suggests that the current surfactant concentration (1.0 wt% of the aqueous phase) was insufficient to stabilize the microspheres generated at a stirring rate of 1500 rpm. Therefore, by varying the stirring rate, three types of aerogel microspheres with remarkable differences in particle sizes were prepared. The physical properties as well as the oil/solvent absorption properties of these three types of microspheres were systematically investigated and discussed below.

Fig. 3 shows the microstructures of the aerogel microspheres with different particle sizes. The spherical aerogel microspheres had a highly porous structure. As shown in Table 1, the particle size decreased from 499 to 53 μm and the pore sizes decreased from 33 to 0.74 μm as the stirring rate increased from 500 to 1000 rpm. The variation of the pore sizes may be attributed to the different freezing rates/times experienced by the aerogel microspheres with different particle sizes. The porous structure of the aerogels was templated from the space occupied by the ice crystals. The sizes of the ice crystals were affected by the freezing rate/time (Oetjen & Haseley, 2004). A faster freezing rate or shorter freezing time typically leads to smaller ice crystals, likely due to a shorter crystal growth period among other possible factors (Oetjen & Haseley, 2004; Zhang & Cooper, 2007). Since the particle sizes of the large microspheres (449 μm) formed at 500 rpm were almost 8.5 times larger than that of the small sized microspheres (53 μm) formed at 1000 rpm, the volume of the corresponding aqueous droplets differed by almost 600 times. Therefore, during the initial freez-

Table 1
The bulk density, BET area, and porosity of the PVA/CNF aerogel microspheres with different particle sizes before and after silane coating.

	Diameter (μm)	Pore Size (μm)	Bulk Density (mg/cm^3)	BET Area (m^2/g)	Porosity (%)
Uncoated Microsphere500	449 ± 64	33 ± 20	4.66 ± 0.11	43.8 ± 4.3	99.7
Coated Microsphere500			5.98 ± 0.10	35.1 ± 2.5	99.6
Uncoated Microsphere750	128 ± 64	7.5 ± 2.6	7.92 ± 0.14	92.8 ± 0.9	99.4
Coated Microsphere750			11.47 ± 0.23	82.8 ± 1.7	99.1
Uncoated Microsphere1000	54 ± 26	0.74 ± 0.29	8.89 ± 0.74	117.0 ± 1.4	99.3
Coated Microsphere1000			16.54 ± 0.61	106.1 ± 1.9	98.7

Table 2
Comparison of the absorption capacities of different materials.

Absorption materials	Absorption Capacity (g/g)	Reference
Silane-coated PVA/CNF aerogel microsphere	54–140	This work
Monolith silane-coated PVA/CNF aerogel	44–96	Zheng et al. (2014) (Our previous work)
Reduced graphene oxide/polyurethane sponge	28–45	Tjandra et al. (2015)
Chitosan/silica composite aerogel	13–30	Ma et al. (2015)
Ethenol-based polymeric microsphere	5–95	Deng et al. (2015)
Graphene-based aerogel	28–40	(Wu et al. (2013)
Spongy graphene	20–86	(Bi et al. (2012)
P(MMA-*co*-PETEA-*co*-BMA)-g-polystyrene	4–21	(Liang et al. (2013)
Modified polyurethane sponge	95–110	(Wu et al. (2014)

ing step before the freeze-drying process, the time required for freezing the smaller aqueous droplets formed under a high stirring rate (e.g., 1000 rpm) was much shorter than that required for freezing the bigger aqueous droplets formed under a low stirring rate (e.g., 500 rpm). A shorter freezing time led to the formation of aerogel microspheres with smaller pore sizes. These variations in the microstructures of the aerogel microspheres led to different physical properties, including differences in the density, BET specific surface area, and oil absorption capacities.

As shown in Table 1, the BET area of the smaller sized microspheres obtained at a higher stirring rate was obviously higher than that of the larger sized microspheres obtained at a lower stirring rate. This phenomenon can be attributed to the pore size differences in these aerogel microspheres. Fig. 3(a_2), (b_2) and (c_2) clearly shows that the larger microspheres exhibited an interconnected porous structure made of large gaps between the cell walls (e.g., Fig. 3a_2), while the smaller microspheres had a porous structure made of numerous tiny pores (e.g., Fig. 3(c_2)). Different from the trend of the BET surface area, the bulk density of the aerogel microspheres decreased as the microsphere size increased, suggesting that the porosity of the larger microspheres was higher than that of the smaller ones. Microspheres with an interconnected

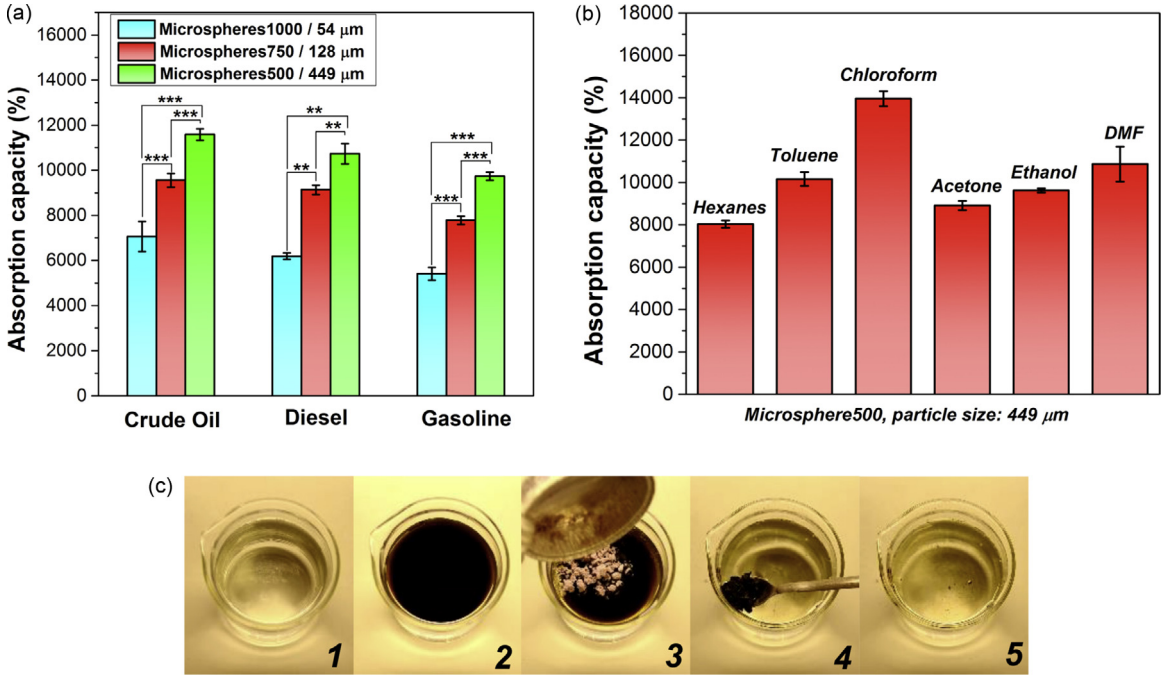

Fig. 6. Testing of the oil/solvent absorption abilities. (a) Absorption capacities of the PVA/CNF aerogel microspheres with different particle sizes for various oils as indicated by weight gain. **: $p < 0.01$; ***: $p < 0.001$. (b) Absorption capacities of the PVA/CNF aerogel microspheres prepared using a stirring speed of 500 rpm for various organic solvents as indicated by weight gain. (c) A layer of crude oil on top of the water was absorbed by the silane-coated PVA/CNF aerogel microspheres. The microspheres infiltrated with crude oil were easily collected and removed from the water.

porous structure and a high porosity are desirable for oil absorption applications. As shown in Table 1, as expected, silane treatment increased the density and reduced the specific surface area of the aerogel microspheres due to the formation of the Si–O–Si coating layer on the surface of aerogel microspheres (Fadeev & McCarthy, 2000; Zhai et al., 2015).

3.5. FTIR analyses on the PVA/CNF aerogel microspheres

The hydrophobic modification of the PVA/CNF aerogel microspheres was achieved via a thermal chemical vapor deposition method. The highly mobile reactive precursor (i.e., methyltrichlorosilane) can easily penetrate through the porous structure and reach the hydroxyl groups present on the surface of the aerogel microspheres. Under a dry reaction condition, methyltrichlorosilane can covalently form a strong cross-linked Si–O–Si monolayer coating by horizontal polymerization of self-assembled silane molecules (Fadeev & McCarthy, 2000). This monolayer coating not only makes the aerogel microsphere hydrophobic, but also enhances the mechanical properties of the aerogel (Zhai et al., 2015). The silane coating layer on the surface of the aerogel microspheres was confirmed by FTIR analyses (Fig. 4). The two absorption bands at ~779 and 1271 cm^{-1} shown in the FTIR spectra were ascribed to the characteristic vibrations of Si–O–Si and C–Si asymmetric stretching, respectively, in the C–Si–O units (Zhu et al., 2013).

3.6. Thermal stability of the PVA/CNF aerogel microspheres

Fig. 5 shows the thermal stability of the PVA/CNF aerogel microspheres (500 and 1000) before and after silane treatment by TGA from 30 °C to 800 °C. The thermal stability of the aerogel microspheres obviously improved after silane treatment. Due to the presence of the Si–O–Si coating layer, the residual weight of the aerogel microspheres before and after silane treatment at 800 °C increased from 6.5% to 18% and 0.2% to 31% for microsphere500 and microsphere1000, respectively. This can be contributed to the weight gain difference of the aerogel microspheres with larger and smaller sizes before and after silane treatment. According to the weight gain of the aerogel microspheres after silane treatment, the weight percentages of the silane coating layer were 22% and 46% for the larger and smaller size microspheres, respectively.

3.7. Evaluation of the oil/solvent absorption capacities and floating oil cleanup ability of the aerogel microspheres

Typical strategies for remediating accidental oil spills include emulsification using dispersants (Ramachandran, Hodson, Khan, & Lee, 2004), absorption using synthetic or natural materials (Wei, Mather, Fotheringham, & Yang, 2003), and direct burning of surface oil (Walton and Mullin, 2003). The absorption of oil spills using natural materials has recently received much attention because it is cheap, effective, and more environmentally friendly (Adebajo et al., 2003). However, natural materials, such as cotton fiber (Deschamps, Caruel, Borredon, Bonnin, & Vignoles, 2003), wool-based nonwoven materials (Radetic et al., 2008), and corn stalks (Husseien, Amer, El-Maghraby, & Hamedallah, 2009), etc., are hydrophilic materials in nature which limit their oil absorption capacities. Materials with a three-dimensional porous structure possess very high oil absorption capacities because the porous structure provides an abundant space for oil uptake (Chu and Pan, 2012). Among the various types of porous materials, those made of biobased and biodegradable materials such as CNFs are most desirable since they are more sustainable and more environmentally friendly (Klemm et al., 2005). Therefore, silane-treated hydrophobic CNF-based aerogels with high porosities can be an ideal material for cleaning up oil/solvent spills from water (Korhonen, Kettunen, Ras, & Ikkala, 2011; Zheng et al., 2014).

The absorption capacities of the silane-coated PVA/CNF aerogel microspheres for different oils were measured and are reported in Fig. 6(a). Three common oils, namely, crude oil, diesel, and gasoline were used for testing the oil absorption capacities of the aerogel microspheres with different particle sizes. The oil absorption capacities of the microspheres ranged from 54 to 116 times their initial weights. It is apparent that the larger microspheres possessed a significantly higher oil absorption capacity (Fig. 6(a)). For example, the crude oil absorption capacity of the 54 μm microspheres was 70 times its own weight, while that of the 449 μm microspheres was 116 times its own weight. The statistical analyses of the oil absorption capacities of the microspheres with different sizes are shown in Fig. 6(a). This can likely be attributed to the fact that the larger microspheres had a higher porosity and a more interconnected porous structure. The solvent absorption capacities of the larger microspheres (449 μm) ranged from 80 to 140 times their own weights as reported in Fig. 6(b). The PVA/CNF aerogel microspheres exhibited much higher oil and solvent absorption capacities than most of the existing oil absorption materials (Table 2) (Bi et al., 2012; Deng, Yang, Chen, & Liang, 2015; Liang, Liu, & Chen, 2013; Ma, Liu, Dong, Wang, & Hou, 2015; Tjandra et al., 2015; Wu, Wu, Yu, Zhang, & Zhu, 2014; Wu et al., 2013; Zheng et al., 2014). Several factors, including extremely high porosities, interconnected pores, and highly hydrophobic aerogel surfaces, may have contributed to the high absorption capacities observed with these aerogel microspheres.

3.8. Floating oil cleanup ability of the PVA/CNF aerogel microspheres

The ability of the PCA/CNF aerogel microspheres for floating oil cleanup was also tested by using the microspheres to absorb a layer of floating crude oil on water. As shown in Fig. 6(c), a layer of crude oil (~2500 mg) was poured into a beaker which was pre-filled with water. The silane-coated aerogel microsphere powder (~60 mg) was then added on top of the oil layer. The crude oil was totally absorbed in 40 s and the microspheres infiltrated with crude oil could be easily collected and removed from the water (Movie S1 in the ESI). This test indicates that the hydrophobic PVA/CNF aerogel microspheres have excellent floating oil clean-up capabilities.

4. Conclusions

Superhydrophobic crosslinked PVA/CNF aerogel microspheres were prepared by combining the water-in-oil (W/O) emulsification process and the freeze-drying process, followed by thermal chemical vapor deposition of methyltrichlorosilane. The oil phase required by the emulsification process was conveniently removed through a simple filtration process before the freeze-drying process through judicious selection of the oil phase as well as the cooling agent used in the initial emulsion freezing step prior to freeze-drying. The aerogel microspheres had ultra-low densities ranging from 4.66 to 16.54 mg/cm^3. The effects of the emulsifier concentration, stirring rate, and pH value on the morphology of the aerogel microspheres were carefully studied. The aerogel microspheres prepared at a relatively low stirring rate (e.g., 500 rpm) had a larger particle size, more interconnected pore structure, larger pore size, higher porosity, and higher oil/solvent absorption capacities in comparison with the aerogel microspheres prepared at higher stirring rates. The hydrophobic crosslinked PVA/CNF aerogel microspheres exhibited outstanding oil/solvent absorption capacities and excellent floating oil cleanup property. This study provides a novel approach for the large-scale production of high performance

polymeric aerogel microspheres with controllable morphologies that can be used in a variety of applications.

Acknowledgments

The authors would like to acknowledge the financial support from the University of Wisconsin–Madison, the Wisconsin Institute for Discovery (WID), and the China Scholarship Council (CSC).

Appendix A. Supplementary data

Supplementary data associated with this article can be found, in the online version, at http://dx.doi.org/10.1016/j.carbpol.2016.04.065.

References

Aegerter, M. A., Leventis, N., & Koebel, M. M. (2011). *Aerogels handbook*. London: Springer (Part VII)
Adebajo, M. O., Frost, R. L., Kloprogge, J. T., Carmody, O., & Kokot, S. (2003). Porous materials for oil spill cleanup: a review of synthesis and absorbing properties. *Journal of Porous Materials*, *10*(3), 159–170.
Alnaief, M., Alzaitoun, M. A., Garcia-Gonzalez, C. A., & Smirnova, I. (2011). Preparation of biodegradable nanoporous microspherical aerogel based on alginate. *Carbohydrate Polymers*, *84*(3), 1011–1018.
Antonietti, M., Fechler, N., & Fellinger, T. P. (2014). Carbon aerogels and monoliths: control of porosity and nanoarchitecture via sol-gel routes. *Chemistry of Materials*, *26*(1), 196–210.
Bi, H. C., Xie, X., Yin, K. B., Zhou, Y. L., Wan, S., He, L. B., et al. (2012). Spongy graphene as a highly efficient and recyclable sorbent for oils and organic solvents. *Advanced Functional Materials*, *22*(21), 4421–4425.
Cai, H. L., Sharma, S., Liu, W. Y., Mu, W., Liu, W., Zhang, X. D., et al. (2014). Aerogel microspheres from natural cellulose nanofibrils and their application as cell culture scaffold. *Biomacromolecules*, *15*(7), 2540–2547.
Cay, A., & Miraftab, M. (2013). Properties of electrospun poly(vinyl alcohol) hydrogel nanofibers crosslinked with 1,2,3,4-butanetetracarboxylic acid. *Journal of Applied Polymer Science*, *129*(6), 3140–3149.
Chen, W. S., Yu, H. P., Li, Q., Liu, Y. X., & Li, J. (2011). Ultralight and highly flexible aerogels with long cellulose I nanofibers. *Soft Matter*, *7*(21), 10360–10368.
Chu, Y., & Pan, Q. M. (2012). Three-dimensionally macroporous Fe/C nanocomposites As highly selective oil-Absorption materials. *ACS Applied Materials & Interfaces*, *4*(5), 2420–2425.
Deng, J. P., Yang, B. W., Chen, C., & Liang, J. Y. (2015). Renewable eugenol-Based polymeric oil-Absorbent microspheres: preparation and oil absorption ability. *ACS Sustainable Chemistry & Engineering*, *3*(4), 599–605.
Deschamps, G., Caruel, H., Borredon, M. E., Bonnin, C., & Vignoles, C. (2003). Oil removal from water by selective sorption on hydrophobic cotton fibers. 1. Study of sorption properties and comparison with other cotton fiber-based sorbents. *Environmental Science & Technology*, *37*(5), 1013–1015.
El Kadib, A., & Bousmina, M. (2012). Chitosan bio-based organic-Inorganic hybrid aerogel microspheres. *Chemistry-A European Journal*, *18*(27), 8264–8277.
Fadeev, A. Y., & McCarthy, T. J. (2000). Self-assembly is not the only reaction possible between alkyltrichlorosilanes and surfaces: monomolecular and oligomeric covalently attached layers of dichloro- and trichloroalkylsilanes on silicon. *Langmuir*, *16*(18), 7268–7274.
Feczko, T., Kokol, V., & Voncina, B. (2010). Preparation and characterization of ethylcellulose-based microcapsules for sustaining release of a model fragrance. *Macromolecular Research*, *18*(7), 636–640.
Garcia-Gonzalez, C. A., & Smirnova, I. (2013). Use of supercritical fluid technology for the production of tailor-made aerogel particles for delivery systems. *Journal of Supercritical Fluids*, *79*, 152–158.
Harifi, T., & Montazer, M. (2012). Past, present and future prospects of cotton cross-linking: new insight into nano particles. *Carbohydrate Polymers*, *88*(4), 1125–1140.
Hong, S. K., Yoon, M. Y., & Hwang, H. J. (2012). Synthesis of spherical silica aerogel powder by emulsion polymerization technique. *Journal of Ceramic Processing Research*, *13*, S145–S148.
Husing, N., & Schubert, U. (1998). Aerogels airy materials: chemistry, structure, and properties. *Angewandte Chemie-International Edition*, *37*(1-2), 22–45.
Husseien, M., Amer, A. A., El-Maghraby, A., & Hamedallah, N. (2009). A comprehensive characterization of corn stalk and study of carbonized corn stalk in dye and gas oil sorption. *Journal of Analytical and Applied Pyrolysis*, *86*(2), 360–363.
Kistler, S. S. (1931). Coherent expanded aerogels and jellies. *Nature*, *127*, 741.
Klemm, D., Heublein, B., Fink, H. P., & Bohn, A. (2005). Cellulose: fascinating biopolymer and sustainable raw material. *Angewandte Chemie-International Edition*, *44*(22), 3358–3393.
Klemm, D., Kramer, F., Moritz, S., Lindstrom, T., Ankerfors, M., Gray, D., et al. (2011). Nanocelluloses: a new family of nature-Based materials. *Angewandte Chemie-International Edition*, *50*(24), 5438–5466.
Korhonen, J. T., Kettunen, M., Ras, R. H. A., & Ikkala, O. (2011). Hydrophobic nanocellulose aerogels as floating, sustainable, reusable, and recyclable oil absorbents. *ACS Applied Materials & Interfaces*, *3*(6), 1813–1816.
Liang, Y., Liu, D. L., & Chen, H. (2013). Poly(methyl methacrylate-co-pentaerythritol tetraacrylate-co-butyl methacrylate)-g-polystyrene: synthesis and high oil-absorption property. *Journal of Polymer Science Part A-Polymer Chemistry*, *51*(9), 1963–1968.
Liu, N., Zhang, S. T., Fu, R. W., Dresselhaus, M. S., & Dresselhaus, G. (2006). Carbon aerogel spheres prepared via alcohol supercritical drying. *Carbon*, *44*(12), 2430–2436.
Lund, K., & Brelid, H. (2013). Kinetics of cross-Linking softwood kraft pulp with 1,2,3,4-butanetetracarboxylic acid. *Industrial & Engineering Chemistry Research*, *52*(33), 11502–11509.
Ma, Q., Liu, Y. F., Dong, Z., Wang, J. L., & Hou, X. (2015). Hydrophobic and nanoporous chitosan-silica composite aerogels for oil absorption. *Journal of Applied Polymer Science*, *132*(15).
Moon, R. J., Martini, A., Nairn, J., Simonsen, J., & Youngblood, J. (2011). Cellulose nanomaterials review: structure, properties and nanocomposites. *Chemical Society Reviews*, *40*(7), 3941–3994.
Oetjen, G.-W., & Haseley, P. (2004). *Freeze-drying*. Weinheim: Wiley-VCH.
Okubo, M., Katayama, Y., & Yamamoto, Y. (1991). Studies on suspension and emulsion.121. Preparation of micron-Size monodisperse polymer microspheres having cross-Linked structures and vinyl groups. *Colloid and Polymer Science*, *269*(3), 217–221.
Okubo, M., Shiozaki, M., Tsujihiro, M., & Tsukuda, Y. (1991). Studies on suspension and emulsion.122. Preparation of micron-size monodisperse polymer particles by seeded polymerization utilizing the dynamic monomer swelling method. *Colloid and Polymer Science*, *269*(3), 222–226.
Radetic, M., Ilic, V., Radojevic, D., Miladinovic, R., Jocic, D., & Jovancic, P. (2008). Efficiency of recycled wool-based nonwoven material for the removal of oils from water. *Chemosphere*, *70*(3), 525–530.
Ramachandran, S. D., Hodson, P. V., Khan, C. W., & Lee, K. (2004). Oil dispersant increases PAH uptake by fish exposed to crude oil. *Ecotoxicology and Environmental Safety*, *59*(3), 300–308.
Saito, T., Hirota, M., Tamura, N., Fukuzumi, H., & Isogai, A. (2009). Individualization of nanosized plant cellulose fibrils achieved by TEMPO-mediated oxidation under neutral conditions. *Abstracts of Papers of the American Chemical Society*, 237.
Saito, T., Kimura, S., Nishiyama, Y., & Isogai, A. (2007). Cellulose nanofibers prepared by TEMPO-mediated oxidation of native cellulose. *Biomacromolecules*, *8*(8), 2485–2491.
Su, Y. Z., Zhang, Y., Zhuang, X. D., Li, S., Wu, D. Q., Zhang, F., et al. (2013). Low-temperature synthesis of nitrogen/sulfur co-doped three-dimensional graphene frameworks as efficient metal-free electrocatalyst for oxygen reduction reaction. *Carbon*, *62*, 296–301.
Tjandra, R., Lui, G., Veilleux, A., Broughton, J., Chiu, G., & Yu, A. P. (2015). Introduction of an enhanced binding of reduced graphene oxide to polyurethane sponge for oil absorption. *Industrial & Engineering Chemistry Research*, *54*(14), 3657–3663.
Vazhayal, L., Talasila, S., Azeez, P. M. A., & Solaiappan, A. (2014). Mesochanneled hierarchically porous aluminosiloxane aerogel microspheres as a stable support for pH-responsive controlled drug release. *ACS Applied Materials & Interfaces*, *6*(17), 15564–15574.
Walton, W. D., & Mullin, J. V. (2003). NIST SP 995 in situ burning of oil spills: resource collection 2CD ROM set. *Spill Science & Technology Bulletin*, *8*(4), 405–406.
Wei, Q. F., Mather, R. R., Fotheringham, A. F., & Yang, R. D. (2003). Evaluation of nonwoven polypropylene oil sorbents in marine oil-spill recovery. *Marine Pollution Bulletin*, *46*(6), 780–783.
Wu, D. C., Xu, F., Sun, B., Fu, R. W., He, H. K., & Matyjaszewski, K. (2012). Design and preparation of porous polymers. *Chemical Reviews*, *112*(7), 3959–4015.
Wu, D. D., Wu, W. J., Yu, Z. Y., Zhang, C. Y., & Zhu, H. T. (2014). Facile preparation and characterization of modified polyurethane sponge for oil absorption. *Industrial & Engineering Chemistry Research*, *53*(52), 20139–20144.
Wu, T., Chen, M. X., Zhang, L., Xu, X. Y., Liu, Y., Yan, J., et al. (2013). Three-dimensional graphene-based aerogels prepared by a self-assembly process and its excellent catalytic and absorbing performance. *Journal of Materials Chemistry A*, *1*(26), 7612–7621.
Wu, Z. S., Yang, S. B., Sun, Y., Parvez, K., Feng, X. L., & Mullen, K. (2012). 3D nitrogen-doped graphene aerogel-supported Fe3O4 nanoparticles as efficient eletrocatalysts for the oxygen reduction reaction. *Journal of the American Chemical Society*, *134*(22), 9082–9085.
Yavari, F., Chen, Z., Thomas, A. V., Ren, W., Cheng, H.-M., & Koratkar, N. (2011). High sensitivity gas detection using a macroscopic three-dimensional graphene foam network. *Scientific Reports*, *1*, 166.
Yun, S., Luo, H. J., & Gao, Y. F. (2014). Superhydrophobic silica aerogel microspheres from methyltrimethoxysilane: rapid synthesis via ambient pressure drying and excellent absorption properties. *RSC Advances*, *4*(9), 4535–4542.
Zhai, T. L., Zheng, Q. F., Cai, Z. Y., Turng, L. S., Xia, H. S., & Gong, S. Q. (2015). Poly(vinyl alcohol)/cllulose nanofibril hybrid aerogels with an aligned microtubular porous structure and their composites with polydimethylsiloxane. *ACS Applied Materials & Interfaces*, *7*(13), 7436–7444.

Zhang, H., & Cooper, A. I. (2007). Aligned porous structures by directional freezing. *Advanced Materials*, *19*(11), 1529–1533.
Zheng, Q. F., Cai, Z. Y., & Gong, S. Q. (2014). Green synthesis of polyvinyl alcohol (PVA)-cellulose nanofibril (CNF) hybrid aerogels and their use as superabsorbents. *Journal of Materials Chemistry A*, *2*(9), 3110–3118.
Zheng, Q. F., Cai, Z. Y., Ma, Z. Q., & Gong, S. Q. (2015). Cellulose nanofibril/reduced graphene Oxide/Carbon nanotube hybrid aerogels for highly flexible and all-Solid-State supercapacitors. *ACS Applied Materials & Interfaces*, *7*(5), 3263–3271.
Zhu, Q., Chu, Y., Wang, Z. K., Chen, N., Lin, L., Liu, F. T., et al. (2013). Robust superhydrophobic polyurethane sponge as a highly reusable oil-absorption material. *Journal of Materials Chemistry A*, *1*(17), 5386–5393.